

LETTER • OPEN ACCESS

Oxygen-incorporated single-photon sources observed at the surface of silicon carbide crystals

To cite this article: Yasuto Hijikata *et al* 2018 *J. Phys. Commun.* **2** 111003

View the [article online](#) for updates and enhancements.



LETTER

OPEN ACCESS

RECEIVED

18 June 2018

REVISED

21 August 2018

ACCEPTED FOR PUBLICATION

2 November 2018

PUBLISHED

14 November 2018

Original content from this work may be used under the terms of the [Creative Commons Attribution 3.0 licence](#).

Any further distribution of this work must maintain attribution to the author(s) and the title of the work, journal citation and DOI.



Oxygen-incorporated single-photon sources observed at the surface of silicon carbide crystals

Yasuto Hijikata¹ , Takashi Horii¹, Yoritaka Furukawa², Yu-ichiro Matsushita^{2,4} and Takeshi Ohshima³ ¹ Division of Mathematics Electronics and Information Sciences, Saitama University, Saitama 338-8570, Japan² Department of Applied Physics, The University of Tokyo, Tokyo 113-8656, Japan³ Quantum Beam Science Research Directorate, National Institutes for Quantum and Radiological Science and Technology, Gunma 370-1292, Japan⁴ Present address: Laboratory for Materials and Structures, Tokyo Institute of Technology, Yokohama 226-8503, Japan.E-mail: yasuto@opt.ees.saitama-u.ac.jp**Keywords:** single-photon sources, silicon carbide, semiconductors, single defect, photoluminescence, oxygen isotope

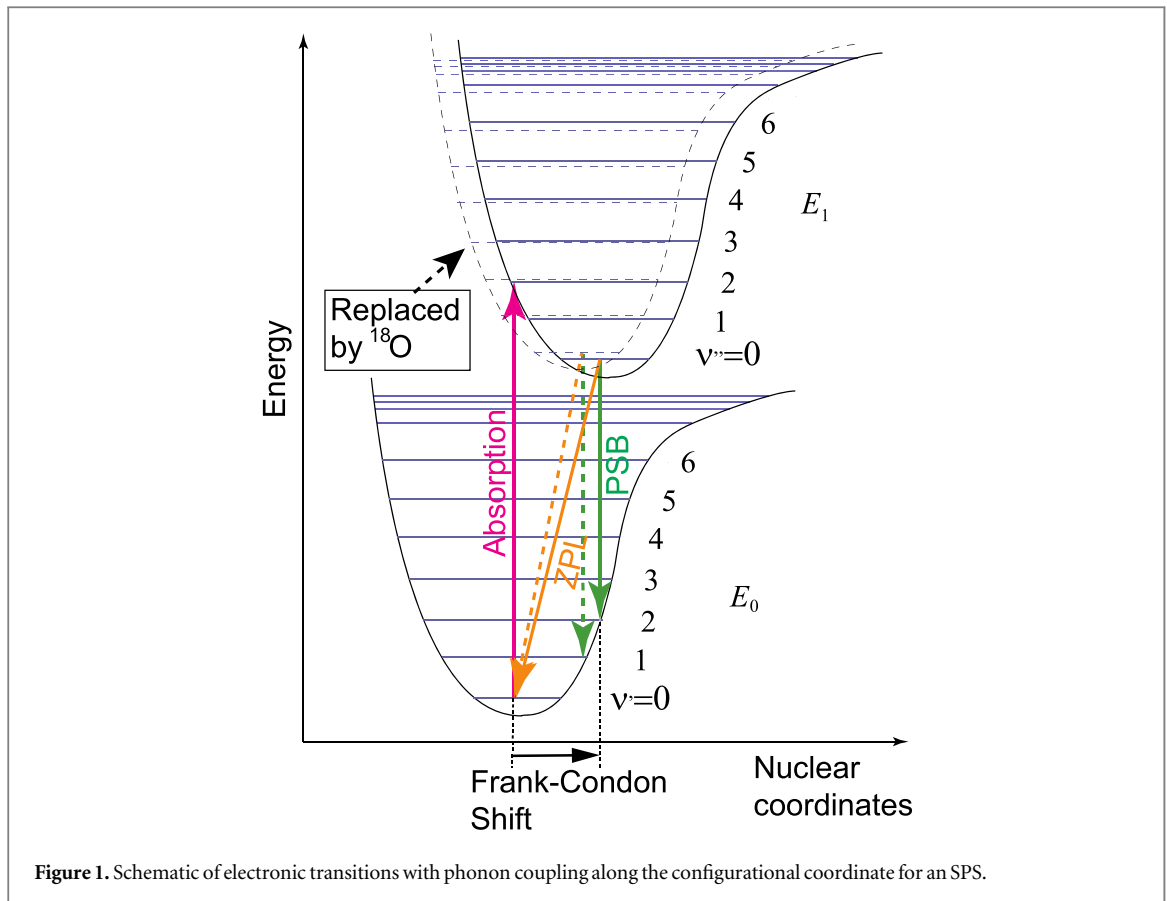
Abstract

The formation of high-brightness single-photon sources (SPSs) that emit single photons at room temperature was recently confirmed in oxygen-annealed SiC semiconductors (surface SPSs.) However, the defect structure of surface SPSs remains unclear, which makes device fabrication and property control difficult. To verify the incorporation of oxygen in surface SPSs, we fabricated SPSs using stable ¹⁸O isotopes as oxidants. By comparing this to the case of natural oxygen annealing, we found that the SP emission spectra for the ¹⁸O sample tended to have shorter peak wavelengths, slightly narrower peak widths, and higher intensities. Thus, it appeared that, in the case of the ¹⁸O sample, the phonon sideband was located closer to the zero-phonon line and that oxygen was incorporated into the defects attributed to the surface SPS.

1. Introduction

Recently, quantum-based technologies such as quantum computing, quantum cryptographic communication, and quantum sensing have led to innovative advances. Single-photon sources (SPSs) that are indispensable to this field have been developed in various materials. Silicon carbide (SiC) is one of the most promising SPS host materials because high-quality and large-diameter wafers are in mass production and various device processes are matured. In addition, several kinds of stable and high-brightness SPSs have been identified at room temperature [1–4], which will enable us to construct quantum devices for practical use. Furthermore, MEMS technologies for SiC enable us to significantly enhance the SP emission rate by introducing an optical resonator around the SPS [5, 6].

It has been reported that high-brightness SPSs (hereafter ‘surface SPSs’) are formed in the vicinity of the SiC-SiO₂ interface upon oxygen annealing of SiC [7]. In addition to room-temperature photo-excited SP emission, electrical-current-excited SP emission at room temperature was also demonstrated from surface SPSs embedded in a *pn* junction diode [4, 8], which is the first achievement after the diamond NV center [9]. However, there are some issues to be resolved, such as the broad emission spectrum and dispersive emission wavelengths of 600–800 nm from the surface SPSs. With the defect structure of the surface SPSs still unclear, it is difficult for us to address these issues. Furthermore, even the presence of electron spin in surface SPSs has not yet been demonstrated. Thus, it is important to elucidate the defect structure of surface SPSs. On the other hand, given that the polarization of the SP emission agrees with the crystallographic symmetry of the SiC substrate [7], surface SPSs are located near the SiC-SiO₂ interface but completely inside the SiC crystal. Therefore, since the defect structure is likely complex (i.e., a point defect pair), the broad spectrum is presumably due to the wide phonon sideband (PSB) emission, as in the case of diamond NV centers. In addition, Lohrmann *et al* suggested that the single defects attributed to surface SPSs were carbon- or oxygen-related defects because they exhibited



similar behavior, even though they were formed in different polytypes having different bandgaps [7]. We speculate that the inclusion of oxygen is more likely for a surface SPS because carbon-related defects are usually not single-photon sources (e.g., C vacancies [10], D1 centers [11].) The use of an oxygen marker such as a stable oxygen isotope (^{18}O) may help to settle this issue. On the other hand, Lohrmann *et al* also suggested that the variation in emission wavelength is due to the variation in the distance between surface SPSs and stacking faults, because the presence of stacking faults produces a linear change in the defect levels of surface SPSs, as shown by *ab initio* studies [4]. Since, as proposed by Matsushita and Oshiyama [12], the SiC-SiO₂ interface may include many stacking faults, it is thought that stacking faults can account for this wavelength variation. A further discussion on the wavelength variation in surface SPSs can be found elsewhere [13].

It is well known that the optical transitions for color centers such as SPSs obey the Frank-Condon principle [14, 15]. Figure 1 shows the coordinate diagram for a color center; E_0 and E_1 denote the energy diagrams for the ground state and excited state, respectively, and ν' and ν'' are the phonon quantum numbers for these states. In general, when an electron is excited from E_0 to E_1 , nuclear coordinate of the E_1 state shifts owing to the Coulomb force of the excited electron (so-called 'Frank-Condon shift'). Since such a nuclear displacement occurs much more slowly than electron transitions, photon absorption (emission) entails phonon absorption (generation) before the recovery of nuclear displacement. Thus, if we employ stable ^{18}O isotopes, which are heavier than natural oxygen (^{16}O), the Frank-Condon shift should decrease, as should the phonon energies, resulting in a shift of PSB toward the zero-phonon line (ZPL) or in a disappearance of PSB. Moreover, the transition energy of the ZPL for ^{18}O might be higher than that for ^{16}O because the degree of change in structural relaxation after electronic excitation is presumably smaller owing to the heavier mass of ^{18}O and the E_1 of the ^{18}O is higher than the E_1 of the ^{16}O .¹³ Thus, by replacing ^{16}O with ^{18}O , we may be able to determine whether the defects attributed to the surface SPS contain oxygen.

In this study, we fabricated three types of samples: Ar-, $^{16}\text{O}_2$ - and $^{18}\text{O}_2$ -annealed. By comparing the radiation properties of these samples, we attempted to determine whether the generation of the surface SPS requires oxidation and the single defects attributed to the surface SPS contain oxygen.

2. Materials and methods

Epitaxial *n*-type 4H-SiC wafers with a 4° off-oriented (0001) Si-face and a net donor concentration $N_d - N_a$ of $1.6 \times 10^{16} \text{ cm}^{-3}$ were used in this study. The samples were oxidized in an infrared furnace at 800 °C in a dry

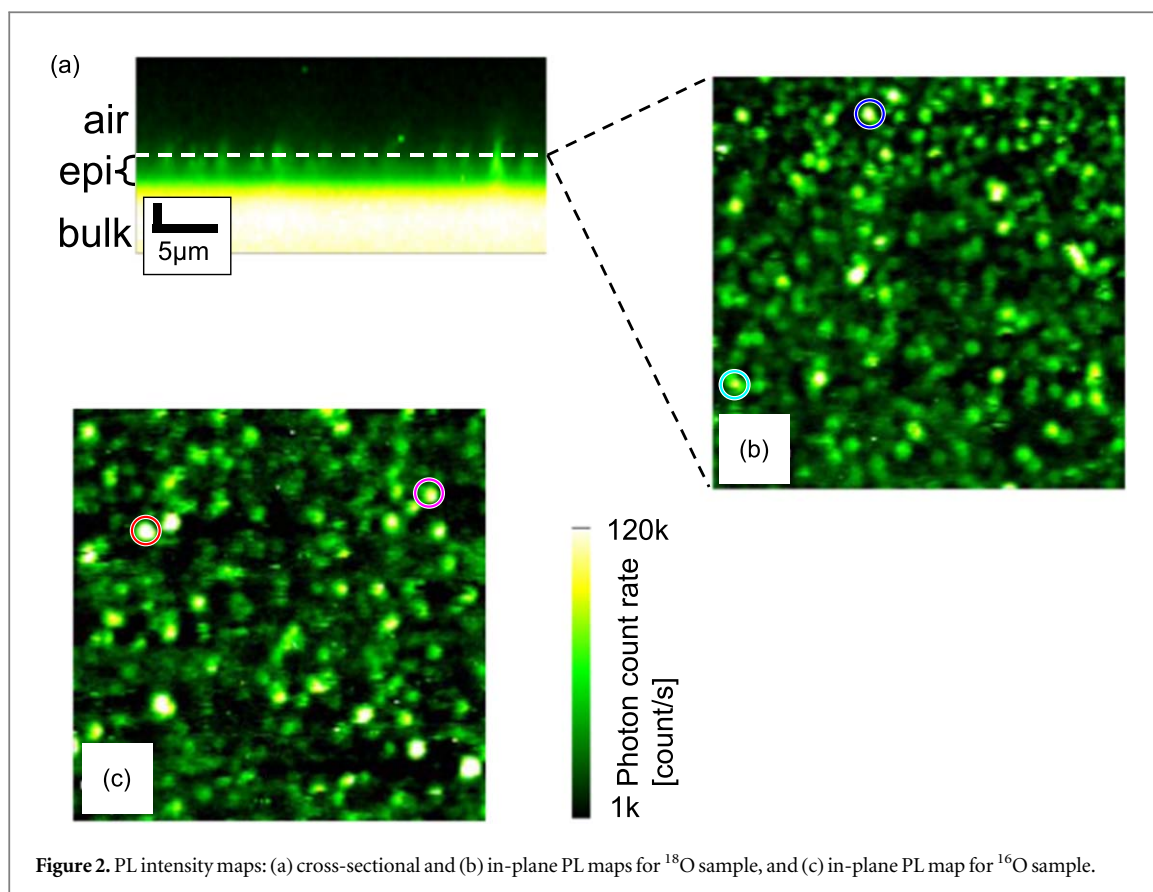


Figure 2. PL intensity maps: (a) cross-sectional and (b) in-plane PL maps for ^{18}O sample, and (c) in-plane PL map for ^{16}O sample.

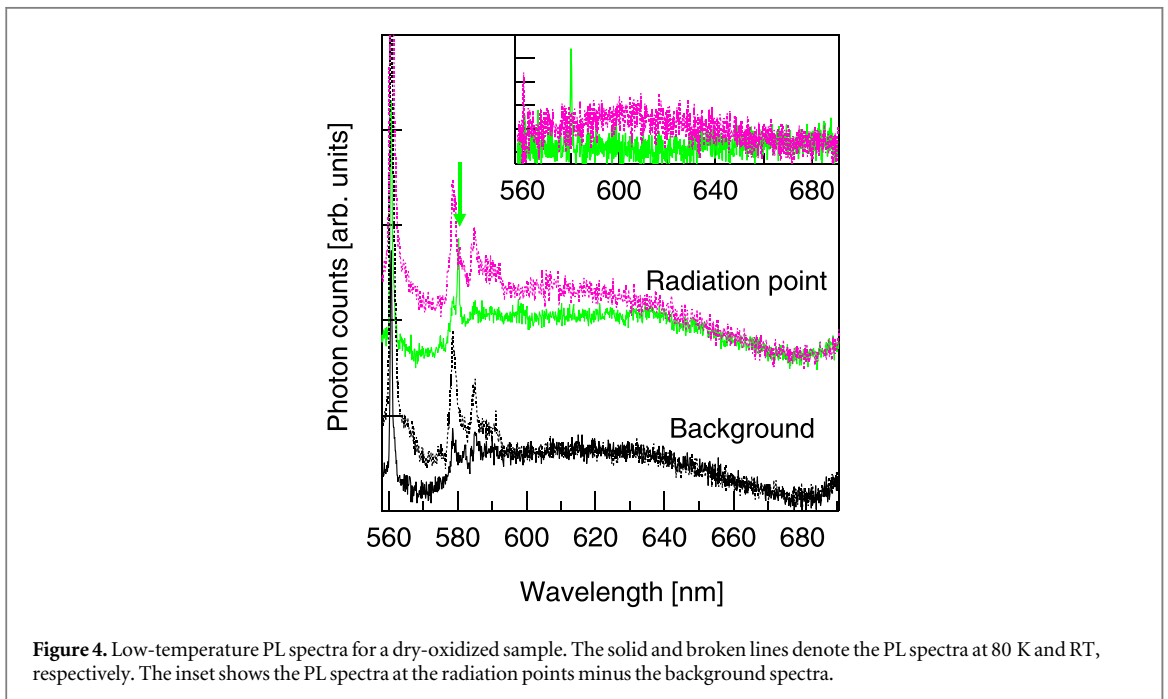
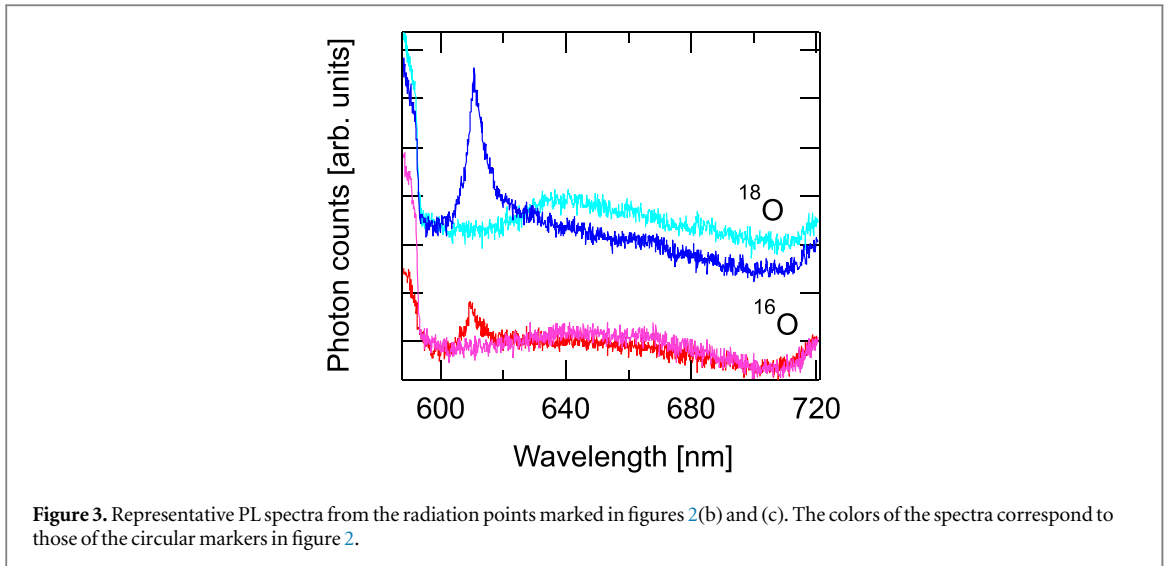
natural or stable-isotope oxygen ($^{16}\text{O}_2/^{18}\text{O}_2$) atmosphere at 5 Pa for 30 min. Another specimen was annealed in an Ar atmosphere at 800 °C and 100 kPa for 30 min. Photoluminescence (PL) from the samples was observed using a confocal laser scanning fluorescence microscope (CFM) (WITec) with an NA0.9 100 × air objective lens (Nikon), single-photon counting modules (Laser Components), and a spectrometer with a CCD detector (Princeton Instruments). The measurement durations of the photon counter and spectrometer were 0.01 s and 0.1 s, respectively. A DPSS laser with a 532-nm wavelength and 1-mW net output was used on the sample as an excitation source. During PL intensity mapping and photon correlation measurements, a 600-nm long-pass filter was placed in front of the photon counter. Low-temperature PL measurements were performed by cooling the sample mounted in a vacuum chamber with a liquid N_2 flow. Photon correlation measurements were performed with a standard Hanbury-Brown-Twiss interferometer.

3. Results and discussion

First, we carried out PL intensity mapping for the Ar-annealed sample. There were numerous radiation points on the in-plane PL map of the sample surface (not shown here). Next, we randomly selected 68 radiation points and performed photon correlation measurements on each. We found that none of them exhibited anti-bunching characteristics. Thus, we concluded that a surface SPS cannot be generated only by heating a SiC substrate. It is known that Ar annealing of SiC substrates often produces carbon byproducts, such as graphitic C [16] and C clusters [17]. Therefore, carbon-related defects can be ruled out as a candidate for surface SPSs.

Figures 2(a) and (b) show cross-sectional and in-plane PL maps of the ^{18}O sample, respectively, and 2(c) shows an in-plane PL map of the ^{16}O sample. As shown in the figure, several dozen radiation points were observed on each sample surface, i.e., the SiC-oxide interfaces. Figure 3 shows representative PL spectra from the radiation points marked in figures 2(b) and (c). The peak around 590 nm appearing in all the spectra is the second-order Raman shift from the 4H-SiC substrate [18]. It was found that there were two kinds of spectra for both samples: one with a sharp peak and the other with a broad peak, similar to a previous study [19].

Figure 4 shows the low-temperature PL spectra from a typical radiation point at specimen temperatures of 80 K and RT. The sample used here was fabricated by oxidization in a dry natural-oxygen ambient at 800 °C. The twin peaks in the 580–590 nm range and the intense peaks at 560 nm, observed in all spectra, were due to the above mentioned second-order Raman shift and the LO phonon line, respectively. The low-temperature PL spectrum at the radiation point exhibits a very sharp peak at 580 nm, while a broad peak is observed around

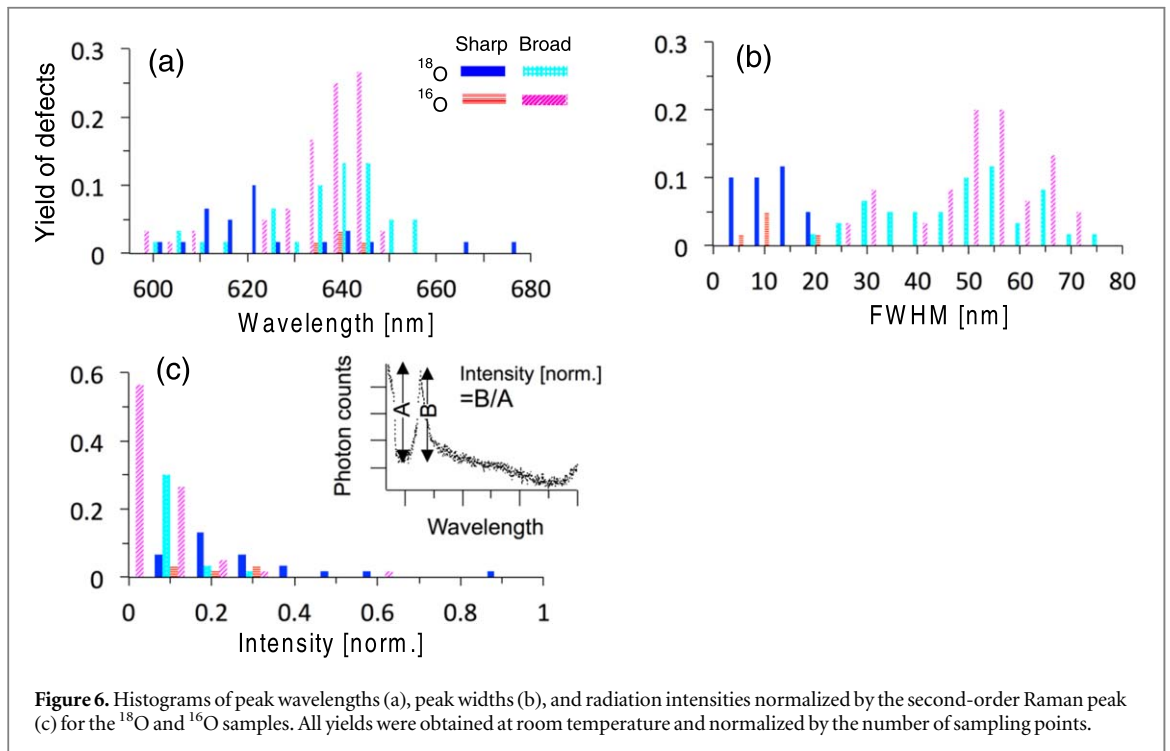
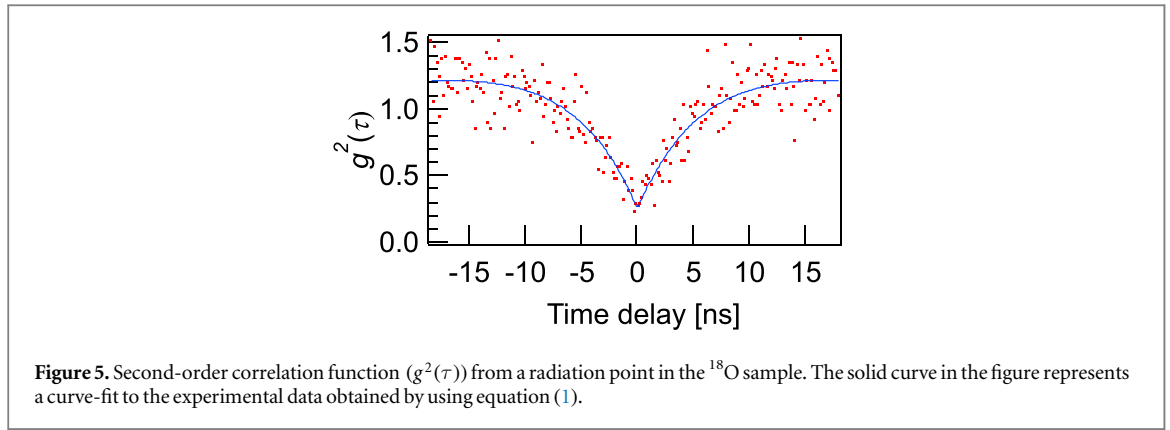


610 nm at RT. The spectra in the inset of figure 4, derived by subtracting the background spectrum, also indicate that the broad peak at RT is red-shifted from the sharp peak at 80 K. Thus, the broad peak observed at RT is entirely composed of PSB, which is observed as the ZPL solely at 80 K. This interpretation corroborates a previous study [20] but contradicts another study [21]. This will be discussed further in a future report.

To determine whether the radiation points corresponded to an SPS, photon correlation measurements were carried out for the ^{16}O and ^{18}O samples. The result for the ^{18}O sample is shown in figure 5. The second-order correlation function $g^2(\tau)$ can be expressed as

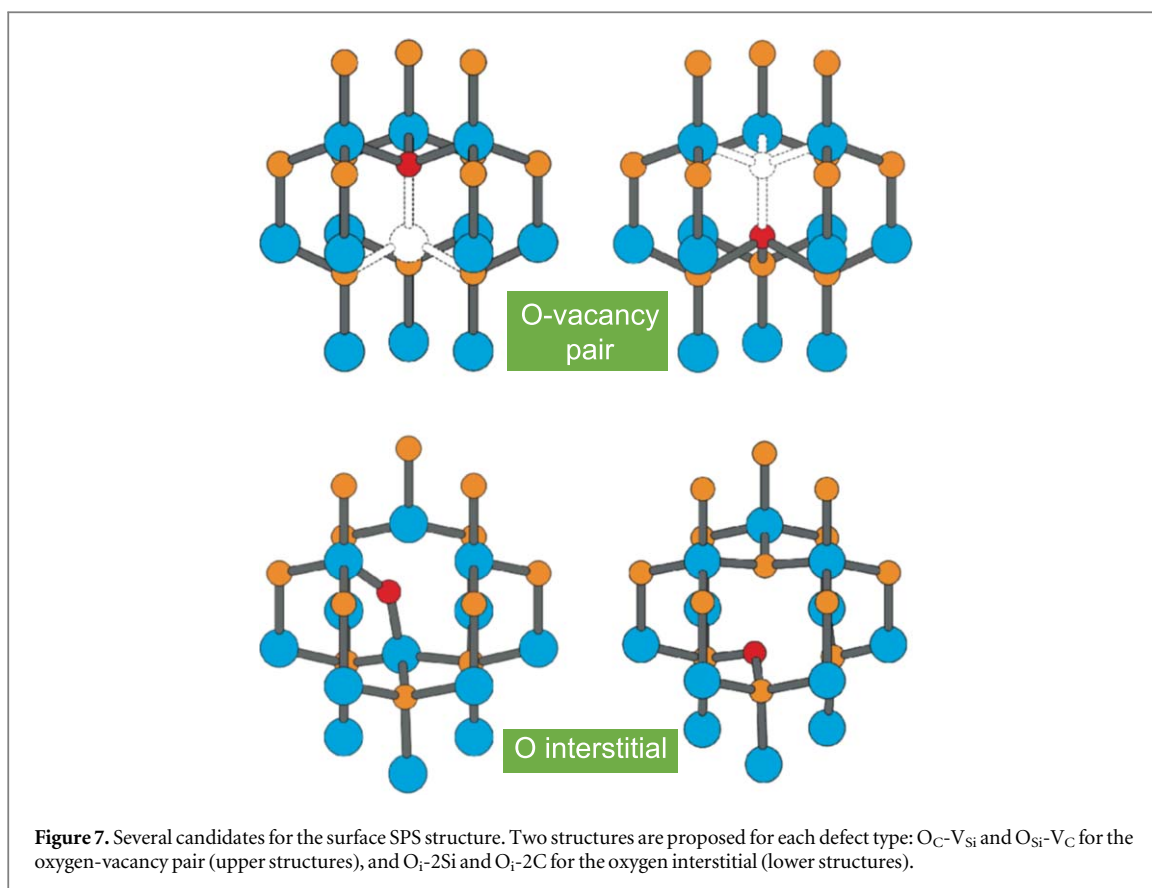
$$g^2(\tau) = 1 + g_f^2 \left\{ -(1 + \alpha) e^{-\frac{|\tau|}{\tau_1}} + \alpha e^{-\frac{|\tau|}{\tau_2}} \right\}, \quad (1)$$

where g_f^2 is the degree of purity of the SP emission. The condition $0.5 \leq g_f^2 \leq 1$ corresponds to SPS, α is the extent of transition to the metastable state, and τ_i ($i = 1$ and 2 for anti-bunching and bunching, respectively) is the radiation lifetime. The solid curve in figure 5 represents a fit to the experimental data obtained by using equation (1). From this fit, g_f^2 , α , and τ_1 were found to be 0.685, 1.40, and 5.67 ns, respectively. Thus, this radiation point is clearly an SPS. In addition, the α value suggests that a three-level transition is predominant. It should be noted that the radiation rate $1/\tau_1$, which corresponds to the radiation intensity, is roughly twice that of a diamond NV center [9]. However, the radiation intensity is generally lower than those of the $4H$ -SiC surface SPSs in previous reports [4, 7, 20], which could be attributable to the low-pressure oxidation occurring in the



present case. We also measured the $g^2(\tau)$ for the ^{16}O sample, as well as for other radiation points in the ^{18}O sample. All the results obtained were similar to those shown in figure 5.

We obtained such PL spectra at room temperature from about 60 radiation points for each ^{18}O sample and ^{16}O sample and made histograms of peak wavelengths, peak widths, and radiation intensities to compare these samples (figure 6). The sharp and broad peaks for each sample are distinguished by color. As discussed above, the sharp peak and the broad peak can respectively be regarded as the ZPL alone and the superposition of ZPL and PSB. The radiation intensities were derived from the peak height normalized by the peak height for the second-order Raman shift (see inset in figure 6(c)). Figure 6(a) reveals that the ^{18}O sample tended to have a larger number of sharp peaks, widely distributed between 600 and 680 nm, compared to the ^{16}O sample, which had few sharp peaks, mostly distributed around 640 nm. However, the sharp peaks of the ^{18}O sample were concentrated around 615 nm, which is lower than the 640 nm for the ^{16}O sample. The photon energy difference between 615 nm (2.016 eV) and 640 nm (1.934 eV) roughly corresponds to that of the square root of their masses. Therefore, as mentioned above, the E_1 level of the ^{18}O sample was presumably elevated owing to its heavier mass. In the case of the broad peaks, the peak wavelengths did not differ significantly between the ^{18}O and ^{16}O samples. Figure 6(b) reveals that the broad peaks were slightly narrower in the case of the ^{18}O sample, whereas the sharp peak widths were slightly wider, as can be confirmed from their averages and standard deviations: 50.9 ± 14.3 nm and 55.0 ± 12.7 nm (broad peaks of ^{18}O and ^{16}O , respectively); 14.2 ± 5.3 nm and 13.1 ± 5.9 nm (sharp peaks of ^{18}O and ^{16}O , respectively). Taking the wavelength resolution of the spectrometer and signal-to-noise ratio in experiment into account, the difference in the sharp peak widths is insignificant. It is



also seen from figure 6(c) that the ^{18}O sample has stronger radiation intensities, especially in the case of the broad peak. This means that, in the case of the ^{18}O sample, the PSB disappears or is closer to the ZPL.

To compare the radiation intensities, the polarization of the SP emitter should be considered. Since a surface SPS is probably a complex structure similar to a diamond NV center, it should have linear polarization. However, since the defect structures of the ^{18}O and ^{16}O samples are presumably the same, we ignored the influence of polarization on the statistics of the radiation intensity data.

Our experimental results strongly support the presence of oxygen in the single defects attributed to surface SPSs. Next, we consider the candidates for the surface SPS. As mentioned in the Introduction section, the structure is thought to be a complex point defect. Thus, as shown in figure 7, several candidates can be inferred for the surface SPS structure. In the upper two structures, an O atom is inserted into the Si (C) site and the neighboring C (Si) is missing, resulting in an O-vacancy pair. Another possibility is that an O atom becomes interstitial, i.e., bonded to Si (C), as shown in the lower two structures in figure 7. In this case, the bond next to the O interstitial may be broken, and the emission wavelength will depend on which bond is broken. By conducting an *ab initio* study of these defects, the defect structure of the surface SPS can be determined from the calculated defect levels. We are currently also performing first-principles calculations and will be presenting the results elsewhere [13].

4. Conclusions

We investigated the radiation properties of the radiation points formed by Ar annealing, ^{16}O oxidation, and ^{18}O oxidation, to determine whether formation of surface SPSs requires oxidation and whether the defects attributed to surface SPSs contain oxygen. For the Ar-annealed sample, there were no SPSs among the 68 radiation points. This indicates that thermal treatment is insufficient and that oxidation is needed to form surface SPSs. Thus, carbon-related defects could be ruled out as candidates. The radiation spectra showed that the ^{18}O -oxidized sample tended to have a greater number of sharp peaks, smaller sharp peak wavelengths, slightly narrower broad peaks, and stronger intensities as compared to the ^{16}O -oxidized sample. These results revealed that in the case of the ^{18}O sample, the zero-phonon lines on the shorter wavelength side were easier to generate and that the location of the phonon-side band was closer to the zero-phonon line because of the larger mass of ^{18}O , evidencing the incorporation of oxygen in the defects attributed to surface SPSs. Finally, we proposed some

candidate defect structures for surface SPSs to determine whether there is an electron spin and to establish a control method for SP emission from surface SPSs.

Acknowledgments

This work was supported in part by Grants-in-Aid for Scientific Research (15H03967, 17H01056, 18H03770) from the Japan Society for the Promotion of Science.

ORCID iDs

Yasuto Hijikata  <https://orcid.org/0000-0002-6314-0401>

Yu-ichiro Matsushita  <https://orcid.org/0000-0002-9254-5918>

Takeshi Ohshima  <https://orcid.org/0000-0002-7850-3164>

References

- [1] Castelletto S, Johnson B C, Ivády V, Stavrias N, Umeda T, Gali A and Ohshima T 2014 A silicon carbide room-temperature single-photon source *Nat. Mater.* **13** 151–6
- [2] Fuchs F, Stender B, Trupke M, Simin D, Pflaum J, Dyakonov V and Astakhov G V 2015 Engineering near-infrared single-photon emitters with optically active spins in ultrapure silicon carbide *Nat. Commun.* **6** 7578
- [3] Kraus H *et al* 2017 Three-dimensional proton beam writing of optically active coherent vacancy spins in silicon carbide *Nano Lett.* **17** 2865–70
- [4] Lohrmann A, Iwamoto N, Bodrog Z, Castelletto S, Ohshima T, Karle T J, Gali A, Prawer S, McCallum J C and Johnson B C 2015 Single-photon emitting diode in silicon carbide *Nat. Commun.* **6** 8783
- [5] Widmann M *et al* 2015 Coherent control of single spins in silicon carbide at room temperature *Nat. Mater.* **14** 164–8
- [6] Calusine G, Politi A and Awschalom D D 2016 Cavity-enhanced measurements of defect spins in silicon carbide *Phys. Rev. Appl.* **6** 014019
- [7] Lohrmann A, Pezzagna S, Dobrinets I, Spinichelli P, Jaxques V, Roch J-F, Meijer J and Zaitsev A M 2011 Diamond based light-emitting diode for visible single-photon emission at room temperature *Appl. Phys. Lett.* **99** 251106
- [8] Fuchs F, Soltamov V A, Váth S, Baranov P G, Mokhov E N, Astakhov G V and Dyakonov V 2013 Silicon carbide light-emitting diode as a prospective room temperature source for single photons *Sci. Rep.* **3** 1637
- [9] Mizuochi N *et al* 2012 Electrically driven single-photon source at room temperature in diamond *Nat. Photonics* **6** 299–303
- [10] Storasta L and Tsuchida H 2007 Reduction of traps and improvement of carrier lifetime in 4H-SiC epilayers by ion implantation *Appl. Phys. Lett.* **90** 062116
- [11] Storasta L, Carlsson F H C, Sridhara S G, Bergman J P, Henry A, Egilsson T, Halle'n A and Janze'n E 2001 Pseudodonor nature of the D₁ defect in 4H-SiC *Appl. Phys. Lett.* **78** 46–8
- [12] Matsushita Y-i and Oshiyama A 2017 A novel intrinsic interface state controlled by atomic stacking sequence at interfaces of SiC/SiO₂ *Nano Lett.* **17** 6458–63
- [13] Matsushita Y-i Private Communication
- [14] Franck J and Dymond E G 1926 Elementary processes of photochemical reactions *Trans. Faraday Soc.* **21** 536–42
- [15] Condon E A 1926 Theory of intensity distribution in band systems *Phys. Rev.* **28** 1182–201
- [16] Kobayashi H, Sakurai T, Takahashi M and Nishioka Y 2003 Interface states at SiO₂/6H-SiC(0001) interfaces observed by x-ray photoelectron spectroscopy measurements under bias: comparison between dry and wet oxidation *Phys. Rev. B* **67** 115305
- [17] Afanas'ev V V and Stesmans A 1996 Elimination of SiC/SiO₂ interface states by preoxidation ultraviolet-ozone cleaning *Appl. Phys. Lett.* **68** 2141–3
- [18] Burton J C, Sun L, Long F H, Feng Z C and Ferguson I T 1999 First- and second-order Raman scattering from semi-insulating 4H-SiC *Phys. Rev. B* **59** 7282–4
- [19] Tsunemi H, Honda T, Makino T, Onoda S, Sato S-I, Hijikata Y and Ohshima T 2018 Various single photon sources observed in SiC pin diodes *Mater. Sci. Forum* **924** 204–7
- [20] Lienhard B, Schröder T, Mouradian S, Dolode F, Tran T T, Aharonovich I and Englund D 2016 Bright and photostable single-photon emitter in silicon carbide *Optica* **3** 768–74
- [21] Abe Y, Umeda T, Okamoto M, Kosugi R, Harada S, Haruyama M, Kada W, Hanaizumi O, Onoda S and Ohshima T 2018 Single photon sources in 4H-SiC metal-oxide-semiconductor field-effect transistors *Appl. Phys. Lett.* **112** 031105